Hund's Paradox and the Collisional Stabilization of Chiral Molecules

Johannes Trost and Klaus Hornberger

Arnold Sommerfeld Center for Theoretical Physics, Ludwig-Maximilians-Universität München, Theresienstraße 37, 80333 Munich, Germany

(Received 13 November 2008; published 10 July 2009)

We identify the dominant collisional decoherence mechanism which serves to stabilize and superselect the configuration states of chiral molecules. A high-energy description of this effect is compared to the results of the exact molecular scattering problem, obtained by solving the coupled-channel equations. It allows us to predict the experimental conditions for observing the collisional suppression of the tunneling dynamics between the left- and the right-handed configuration of D_2S_2 molecules.

DOI: 10.1103/PhysRevLett.103.023202 PACS numbers: 34.10.+x, 03.65.Xp, 03.65.Yz, 34.20.Gj

Introduction.—An old problem in molecular quantum mechanics, first discussed by Hund [1], is how to explain from first principles why molecules often appear as *enantiomers*, i.e., either in a left-handed configuration or as the right-handed mirror image. Given the parity-invariant molecular Hamiltonian, one might rather expect them in the ground state, corresponding to the symmetric superposition of these chiral states. Traditionally, this is explained by the possibly very long tunneling time from a left-handed configuration state $|L\rangle$ to a right-handed one $|R\rangle$. However, this does not solve the "paradox" since one still needs to understand the seeming failure of the superposition principle, prohibiting superposition states of the form $|\psi_\xi\rangle = (|L\rangle + e^{i\pi\xi}|R\rangle)/\sqrt{2}$ with $0 \le \xi < 2$ [2,3].

While this superselection phenomenon has been linked with fundamental parity violations [4], a very natural explanation is offered by the concept of environmental decoherence [5]. What selects the enantiomer states according to this theory is the fact that the typical interaction with environmental degrees of freedom, such as the collision with a gas particle, can better distinguish the alternatives $|L\rangle$ and $|R\rangle$ than, say, between the molecular eigenstates $|\psi_0\rangle$ and $|\psi_1\rangle$. The enantiomer states are then prevented both from tunneling between each other and from decaying into a mixture, if these environmental interactions are sufficiently frequent compared to the tunneling period. This stabilization can be understood in analogy to the quantum Zeno effect if one views the environment as continuously monitoring the molecular state. Superposition states $|\psi_\xi\rangle$, in contrast, would get quickly decohered by their ensuing quantum correlation with the environment.

This environmental distinction of specific molecular configurations is one of the paradigms in the field of decoherence, discussed by many of the path-breaking works [2,3,6]. At the same time, not much is known about the concrete microscopic mechanism at work with realistic molecules nor whether the transition from the tunneling regime to stabilization can be observed experimentally.

In this Letter, we use the molecular scattering theory to identify the dominant microscopic mechanism responsible for chiral stabilization due to a background gas. We show that this effect is determined by a parity-sensitive higher-order term in the dispersive interaction, which is usually disregarded because it does not affect the equilibrium properties of gases (due to the orientational averaging involved). In spite of this, and in spite of the fact that this process cannot be used to separate a racemic mixture into chiral components, it provides a surprisingly efficient channel for environmental decoherence. This is demonstrated numerically by solving the full-fledged coupled-channel problem for a simple chiral molecule, D_2S_2. Our numerical results motivate and confirm a high-energy approximation, which allows us to assess the decoherence effect at room temperature and to predict when the collision-induced transition from tunneling to stabilized chiral states can be observed experimentally.

Master equation for collisional stabilization.—The following microscopic analysis is facilitated by the recent derivation of a master equation yielding the incoherent dynamics of the internal-rotational molecular state due to the collisions with a lighter, thermalized background gas [7,8]. Crucially, this Markovian description incorporates the interaction between the molecule and the gas particle in a nonperturbative fashion, by means of the multichannel scattering amplitudes.

We assume that the kinetic energy transferred in the collisions is sufficiently small compared to both the Born-Oppenheimer barrier separating the enantiomer states and the excitation energies of the electronic and vibrational internal states of the molecule and the gas particle. This is valid in most cases of interest, and it implies that thermally induced transitions between $|L\rangle$ and $|R\rangle$ do not occur. It is then justified to take the interaction operator to be diagonal in the enantiomer basis $\hat{V} = V_L(\hat{\boldsymbol{r}})|L\rangle\langle L| + V_R(\hat{\boldsymbol{r}})|R\rangle\langle R|$, thus restricting the molecular configuration state to a two-dimensional subspace. Here $\hat{\boldsymbol{r}}$

is the interparticle position operator in the body-fixed molecular system; for simplicity, we disregard a possible dependence of $\hat{V}$ on the orientation of the environmental gas particle.

The master equation [8] simplifies considerably under these assumptions. It is formulated in terms of the scattering amplitudes for the channels corresponding to the molecular eigenstates $|\psi_0\rangle$ and $|\psi_1\rangle$. However, since the S matrix for $\hat{V}$ does not couple subspaces of different chiral configurations $\langle L|\hat{S}|R\rangle = \langle R|\hat{S}|L\rangle = 0$, one can express the proper scattering amplitudes as linear combinations of the scattering amplitudes $f^{(L)}$ and $f^{(R)}$ associated to the unitary scattering operators $\langle L|\hat{S}|L\rangle$ and $\langle R|\hat{S}|R\rangle$. The configuration dynamics then no longer depends on the scattering cross section. Rather, it is determined by

$$\eta_{\alpha\alpha_0}(v) = \int \frac{d\boldsymbol{n} d\boldsymbol{n}_0}{8\pi} |f^{(L)}_{\alpha,\alpha_0}(v\boldsymbol{n}, v\boldsymbol{n}_0) - f^{(R)}_{\alpha,\alpha_0}(v\boldsymbol{n}, v\boldsymbol{n}_0)|^2, \tag{1}$$

which may be called a decoherence cross section. Similar to a proper partial cross section, this characteristic area depends on the relative velocity v and on the initial and final internal states of the molecule, labeled by the multi-indices α_0 and α. In the present case, these are the rotation states of an asymmetric top $\alpha = (j, m_j, \tau)$, specified by the total and azimuthal quantum numbers j and m_j, respectively, and the pseudoquantum number τ. Importantly, the decoherence cross section (1) depends on the phase difference of $f^{(L)}$ and $f^{(R)}$. It may thus be quite large even if the corresponding scattering cross sections are identical: $|f^{(L)}|^2 = |f^{(R)}|^2$. The presence of the background gas also gives rise to a coherent modification of the tunneling dynamics, described by the characteristic area $\varepsilon_{\alpha\alpha_0}(v) = \int d\boldsymbol{n} d\boldsymbol{n}_0 \mathrm{Im}[f^{(L)}_{\alpha,\alpha_0}(v\boldsymbol{n}, v\boldsymbol{n}_0) f^{(R)*}_{\alpha,\alpha_0}(v\boldsymbol{n}, v\boldsymbol{n}_0)]/4\pi$.

In the master equation, the areas $\eta_{\alpha\alpha_0}(v)$ and $\varepsilon_{\alpha\alpha_0}(v)$ are multiplied with the current density of the gas particles to yield the decoherence rate γ and the frequency shift ω_x, respectively. Specifically, the decoherence rate is given by

$$\gamma = n_{\mathrm{gas}}\langle v\eta\rangle \equiv n_{\mathrm{gas}} \sum_{\alpha,\alpha_0} w(\alpha_0) \int_0^\infty dv \nu(v) v \eta_{\alpha\alpha_0}(v), \tag{2}$$

where n_{gas} is the number density of the background gas and $\nu(v)$ its velocity distribution. Here, taking the average over the rotational state distribution $w(\alpha_0)$ is an additional approximation, which is well allowed if the rotation frequency is much greater than the tunneling frequency, as is usually the case. The frequency shift $\omega_x = n_{\mathrm{gas}}\langle v\varepsilon\rangle$ is determined by the same average.

The collisional master equation [8] thus reduces to an equation in the $2d$ space spanned by the $|\psi_\xi\rangle = (|L\rangle + e^{i\pi\xi}|R\rangle)/\sqrt{2}$. Denoting the tunneling frequency by ω_z and identifying the energy eigenstates $|\psi_0\rangle$ and $|\psi_1\rangle$ with the eigenvectors of the Pauli matrix $\hat{\sigma}_z$, it takes the form

$$\partial_t \rho = \frac{1}{2i}[\omega_z \hat{\sigma}_z + \omega_x \hat{\sigma}_x, \rho] + \frac{\gamma}{2}(\hat{\sigma}_x \rho \hat{\sigma}_x - \rho). \tag{3}$$

This equation has the remarkable property of stabilizing the enantiomer states $|R\rangle$ and $|L\rangle$, provided $\gamma \gg \omega_z$, i.e., when the decoherence rate is much greater than the tunneling rate. The chiral configuration states decay with the suppressed rate $\omega_z^2/\gamma \ll \gamma$, w_z in this case, while the superposition states $|\psi_\xi\rangle$ decay at least with rate γ [2,3].

The parity-sensitive dispersion interaction.—We now turn to the general van der Waals interaction between two polarizable particles to identify the relevant part that distinguishes a left-handed from a right-handed configuration and thus gives rise to different scattering amplitudes $f^{(L)}$ and $f^{(R)}$. The total London dispersion interaction is conveniently expressed in terms of the frequency-dependent multipole-polarizability tensors of the particles, most prominently those involving virtual electric dipole (ED) and electric quadrupole (EQ) transitions [9]. It is dominated by the standard van der Waals ED-ED/ED-ED interaction, which depends on the interparticle distance r as r^{-6} and is determined by the ED-ED polarizability tensors $\alpha(i\omega)$. This bulk interaction cannot distinguish different chiral configurations since the $\alpha(i\omega)$ are parity-invariant.

Among the chirally sensitive parts of the London dispersion interaction between a chiral and an achiral molecule, the most important contribution is due to the EQ-ED/ED-ED polarizability combination. It has a r^{-7} dependence, and it combines the EQ-ED polarizability tensor $A_{i,jk}(i\omega)$ of the chiral molecule [9] with the ED-ED polarizability of the spherical projectile. One can safely neglect the contributions involving higher-order electric polarizability tensors due to their short-ranged nature; among the contributions involving magnetic susceptibilities, in particular due to magnetic dipole (MD) and magnetic quadrupole (MQ) transitions, the ED-MD/ED-MD vanishes if one molecule is achiral, while the ED-MD/ED-MQ and ED-MD/EQ-MD are suppressed by the square of the fine structure constant [10,11]. Also the (parity-invariant) influence of a small permanent dipole-moment of the chiral molecules can be usually disregarded, since it gets overshadowed by the van der Waals interaction.

We note that the chirally sensitive EQ-ED/ED-ED interaction contribution is usually not accounted for in molecular scattering calculations. This is because its chiral disparity vanishes when averaged over all orientations of the chiral molecule, implying that the cross sections of left- and right-handed molecules are equal. However, such rotational averaging of the coupled-channel equations, which drastically reduces the calculational effort, is not allowed in the present case, since the decoherence cross section (1) crucially depends on the phase differences of the individual scattering amplitudes $f^{(L)}$ and $f^{(R)}$. This phase information is lost at the level of standard scattering cross sections, which indeed remain equal for left- and right-handed molecules.

Solving the coupled-channel equations.—In order to evaluate the scattering amplitudes, one must calculate the scattering matrix S by solving the associated coupled-channel equations [12]. Our system comprises a chiral asymmetric top molecule colliding with a noble gas atom, such that each channel is described by a set of rotational (pseudo)quantum numbers j, m_j, and τ, as well as by the orbital and the total angular momentum ℓ and J, respectively.

The resulting system of differential equations involves infinitely many closed channels and a finite number of asymptotically free, open channels, which scales with the total energy as $E^{3/2}$. When truncating this infinite system, care is needed to ensure that at least all of those closed channels are retained which have an appreciable coupling to the initial state, even if their asymptotic energies lie deeply in the energetically forbidden domain.

Since state-of-the-art numerical program packages for scattering calculations do not accommodate asymmetric molecules with their parity-changing collision dynamics, we developed a numerical method for solving the full quantum mechanical scattering problem (avoiding premature rotational averaging). It is based on the log-derivative algorithm of Johnson [13], and it allows us to ensure the convergence with respect to the truncation of closed channels by adjusting threshold values both for the closed channel energies and for the internal angular momenta to be retained. We checked our program for the case of symmetric top molecules against the numerical package MOLSCAT [14].

Model for D_2S_2.—The transition from tunneling to stabilization is best observed with a molecule of moderate tunneling frequency ω_z. Motivated by recent proposals for enantiomer discrimination [15,16], we focus on D_2S_2, one of the simplest chiral molecules, with $\omega_z/2\pi = 176$ Hz. Since *ab initio* calculations for the dynamic tensors $\alpha(i\omega)$ and $A_{i,jk}(i\omega)$ are not yet feasible for dihydrogendisulfide (nor for any other chiral molecule), we extend the bond increment method [17] for the calculation of static molecular susceptibilities to the dynamic case. As described in Ref. [17], static molecular susceptibility tensors can be calculated as a sum over bond increments associated to the constituent atoms a, which account for the relative positions and orientation of the atoms and their mutual bonds. The bond increments are obtained from *ab initio* values of static molecular susceptibilities of training compounds, which include the D_2S_2 molecule [17]. In a simple extension of this approach, we replace the static values of the constituent atomic susceptibilities by a Drude model $\alpha^{(a)}(i\omega) = \alpha^{(a)}(0)f_a(\omega)$ and $A^{(a)}_{i,jk}(i\omega) = A^{(a)}_{i,jk}(0)f_a(\omega)$, with $f_a(\omega) = \omega_a^2/(\omega_a^2 + \omega^2)$, where ω_a is the first excitation energy, $\omega_D = 0.375$ a.u., and $\omega_S = 0.252$ a.u. [18]. The configuration of D_2S_2 is characterized by the bond lengths $r_{SS} = 2.05$ Å and $r_{SD} = 1.34$ Å, the interbond angle $\angle(DSS) = 100.4°$, the dihedral angle $\angle(DSSD) = 90.3°$, and constants of inertia given in Ref. [19]. We take the background gas to be ground state helium, whose (spherically symmetric) dipole-dipole polarizability is accurately described by a sum of four Lorentzians [20].

Numerical results.—It takes substantial numerical effort to observe the onset of collisional stabilization, since this regime is characterized by a large number of partial waves, while the standard semiclassical approaches for cross sections cannot be applied. Moreover, the number of relevant scattering channels proliferates; at the kinetic energy $E/k_B = 300$ K of the relative motion, about 1.2×10^4 coupled differential equations would have to be solved simultaneously, with as many different initial conditions, for extracting the S matrix in the subspace of a single total angular momentum J.

The upper panel in Fig. 1 presents the exact total scattering cross section σ_{tot} (for kinetic energies up to 10 K), starting from the rotational ground state of D_2S_2, while the lower panel shows the decoherence cross section $\eta_{tot} = \sum_\alpha \eta_{\alpha\alpha_0}$. One observes that a non-negligible effect of collisional stabilization can be expected already for energies well below the threshold for the first channel that directly couples different parity subspaces ($E_{thres}/k_B = 17.5$ K). The decoherence cross section η_{tot} tends to saturate at about $100a_0^2$, corresponding to $\eta_{tot}/\sigma_{tot} \simeq 10\%$ at 10 K—a remarkably large value, given that the chirality distinguishing interaction contributes only weakly to σ_{tot}.

High-energy approximation.—In order to understand this saturation and to assess the stabilizing effect of collisions at larger temperatures, we now consider a high-energy approximation for η_{tot} and σ_{tot}. Since the Born approximation renders the scattering amplitude a linear functional of the potential, it follows immediately from (1) that the asymptotic high-energy behavior

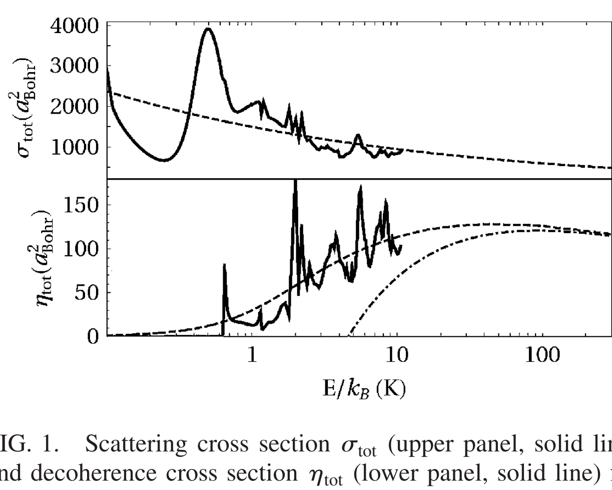

FIG. 1. Scattering cross section σ_{tot} (upper panel, solid line) and decoherence cross section η_{tot} (lower panel, solid line) for the collision of a He atom off a ground state D_2S_2 molecule, as a function of the kinetic energy $E/k_B \leq 10$ K on a logarithmic scale. The dashed line corresponds to (4), and the dashed-dotted line gives the high-energy behavior (5).

of $\eta_{\rm tot}$ is the cross section corresponding to $\Delta V(\boldsymbol{r}) = V_L(\boldsymbol{r}) - V_R(\boldsymbol{r})$. We start from the general dependence of the cross section on the initial state elastic S matrix element $\sigma_{\rm tot} = 2\pi \sum_J (2J+1)[1 - \mathrm{Re}(\langle \Psi_0 | \hat{S}^{(J)} | \Psi_0 \rangle)]/k^2$ [12], apply the exponential Born approximation, and take the high-J asymptotics. For a homogeneous, spherical potential $V(r) = C_n r^{-n}$, this yields the standard result $\tilde{\sigma}^{(n)}_{\rm tot} = p_n (C_n^2/E)^{1/(n-1)}$, with p_n a numerical factor depending weakly on $n > 2$ [12].

Disregarding the molecular core, we can thus approximate $\sigma_{\rm tot}$ by the dominant, spherically symmetric $n = 6$ contribution to the van der Waals ED-ED/ED-ED interaction, i.e., $\sigma_{\rm tot} \simeq \tilde{\sigma}^{(6)}_{\rm tot}$ with $C_6 = 11.7$ a.u. Also, $\Delta V(\boldsymbol{r})$ is homogeneous in r, with $n = 7$, but there is no direct Born contribution to the decoherence cross section $\eta_{\rm tot}$ since $\langle \Psi_0 | \Delta V(\hat{\boldsymbol{r}}) | \Psi_0 \rangle$ vanishes. Therefore, we include all off-diagonal elements that couple the ground state in the exponential Born expression. This yields $\mathrm{Re}(\langle \Psi_0 | \hat{S}^{(J)} | \Psi_0 \rangle) \simeq \cos(\sqrt{\sum_{f \neq 0} |\langle \Psi_0 | \Delta V | \Psi_f \rangle|^2})$, with Ψ_f the free channel wave functions in the J subspace.

The lowest channel Ψ_1 that couples to Ψ_0 via ΔV opens at 17.5 K, with $j = 3$. By expressing the corresponding coupling as $|\langle \Psi_0 | \Delta V | \Psi_1 \rangle| = \hbar^2 \beta^5 / (2 m_* r^7)$, with β a convenient parameterization and m_* the reduced mass, and replacing the sum by an integral, this yields

$$\eta_{\rm tot} \cong \frac{4\pi}{k^2} \int_{1/2}^{\infty} dJ (2J+1) \sin^2 \left\{ \frac{5\pi}{128} (k\beta)^5 \frac{\Gamma(J - \frac{1}{2})}{\Gamma(J + \frac{11}{2})} \right\}, \tag{4}$$

with $E = (\hbar k)^2 / 2m_*$. This approximation is displayed as the dashed line in the lower panel in Fig. 1. The comparison with the exact results indicates that (5) starts to apply already at numerically accessible energies. An asymptotic expansion yields

$$\eta_{\rm tot} \simeq c_1 \frac{\beta^{5/3}}{k^{1/3}} - c_2 \frac{\beta^{5/6}}{k^{7/6}}, \tag{5}$$

with $c_1 = 3.66$ and $c_2 = 14.4$ (see the dashed-dotted line in Fig. 1).

Discussion.—Our numerical and analytical analysis suggests that the ratio $\eta_{\rm tot}/\sigma_{\rm tot}$ varies only weakly at larger energies. A typical value at 300 K of $\eta_{\rm tot}/\sigma_{\rm tot} \simeq 25\%$ means that environmental stabilization sets in once the rate of collisions exceeds 4 times the tunneling frequency. Noting that D_2S_2 tunnels with $\omega_z/2\pi = 176$ Hz, we find from (5) that the critical pressure and temperature of a helium atmosphere must satisfy $(p/\mathrm{mbar})(T/\mathrm{K})^{-2/3} \geq 3.0 \times 10^{-7}$, i.e., $p \geq 1.6 \times 10^{-5}$ mbar for $T = 300$ K.

This prediction could be tested in an experiment that applies laser based coherent control techniques in a Stern-Gerlach-type setup for separating a molecular beam into left- and right-handed daughter beams [15,16]. Passing one of them through a gas cell, one may analyze the enantiomeric purity with another Stern-Gerlach stage. Since thermal racemization can be controlled by cooling (given the 2300 Kk_B barrier height for chiral flipping in D_2S_2), it is thus possible to directly observe the expected environmental stabilization of the chiral configuration as a function of the gas pressure.

This work was supported by the DFG Emmy Noether program.

[1] F. Hund, Z. Phys. **43**, 805 (1927).
[2] M. Simonius, Phys. Rev. Lett. **40**, 980 (1978).
[3] R. A. Harris and L. Stodolsky, J. Chem. Phys. **74**, 2145 (1981); Phys. Lett. **116B**, 464 (1982).
[4] M. Quack, Angew. Chem., Int. Ed. **41**, 4618 (2002).
[5] E. Joos *et al.*, *Decoherence and the Appearance of a Classical World in Quantum Theory* (Springer, Berlin, 2003); W. H. Zurek, Rev. Mod. Phys. **75**, 715 (2003); M. Schlosshauer, *Decoherence and the Quantum-to-Classical Transition* (Springer, Berlin, 2007).
[6] W. H. Zurek, Phys. Rev. D **24**, 1516 (1981); E. Joos and H. D. Zeh, Z. Phys. B **59**, 223 (1985).
[7] R. Dümcke, Commun. Math. Phys. **97**, 331 (1985).
[8] K. Hornberger, Europhys. Lett. **77**, 50 007 (2007).
[9] A. J. Stone, *The Theory of Intermolecular Forces* (Clarendon Press, Oxford, 1996).
[10] Y. N. Chiu, A. V. Kenney, and S. H. Brown, J. Chem. Phys. **73**, 1422 (1980).
[11] J. K. Jenkins, A. Salam, and T. Thirunamachandran, Phys. Rev. A **50**, 4767 (1994).
[12] M. S. Child, *Molecular Collision Theory* (Academic, London, 1984).
[13] B. R. Johnson, J. Comput. Phys. **13**, 445 (1973).
[14] J. M. Hutson and S. Green, MOLSCAT computer code v. 14, Collab. Computat. Project No. 6, EPSRC (United Kingdom).
[15] I. Thanopulos, P. Král, and M. Shapiro, J. Chem. Phys. **119**, 5105 (2003).
[16] Y. Li, C. Bruder, and C. P. Sun, Phys. Rev. Lett. **99**, 130403 (2007).
[17] C. S. Ewig, M. Waldmann, and J. R. Maple, J. Phys. Chem. A **106**, 326 (2002).
[18] *NIST Computational Comparison and Benchmark Handbook*, Number 101, Release 14, edited by R. D. Johnson III (NIST, Gaithersburg, MD, 2006).
[19] G. Winnewisser and K. M. T. Yamada, Vib. Spectrosc. **1**, 263 (1991).
[20] Y. M. Chan and A. Dalgarno, Proc. Phys. Soc. London **86**, 777 (1965).